Entanglement dynamics of the ultrastrong-coupling three-qubit Dicke model

Lijun Mao, Yanxia Liu, and Yunbo Zhang*
Institute of Theoretical Physics, Shanxi University, Taiyuan 030006, People's Republic of China
(Received 12 December 2015; published 3 May 2016)

We give an analytical description of the dynamics of the three-qubit Dicke model using the adiabatic approximation in the parameter regime where the qubit transition frequencies are far off-resonance with the field frequency and the interaction strengths reach the ultrastrong-coupling regimes. Qualitative differences arise upon comparison to single- and two-qubit systems. Simple analytic formulas show that three revival sequences produce a three-frequency beat note in the time evolution of the population. We find an explicit way to estimate the dynamics for qubit-field and qubit-qubit entanglement inside the three-qubit system in the ultrastrong-coupling regime, and the resistance to sudden death proves that the entanglement in the Greenberger-Horne-Zeilinger state is more robust than that in the *W* state.

DOI: 10.1103/PhysRevA.93.052305

I. INTRODUCTION

Recent experimental studies have shown that the ultrastrong-coupling regime, where the coupling strength is some tenths of the mode frequency, can be achieved in a number of implementations such as superconducting circuits [1–4], semiconductor quantum wells [5–7], and possibly also surface acoustic waves [8] and trapped ions [9]. The fast-growing interest in the ultrastrong-coupling regime is motivated not only by theoretical predictions of novel fundamental properties [10–12] but also by potential applications in quantum computing tasks [13,14]. The advent of these impressive experimental results prompts a number of theoretical efforts to find analytical solutions for the quantum Rabi and Dicke models [15,16] by applying various techniques [17–21]. On the other hand, the models are expanded to more general cases, including different qubits [22–26], anisotropic couplings [27–29], a finite-size ensemble of interacting qubits [30], and two-photon interactions [31], to name just a few.

In particular, people start to tackle the entanglement features both between the qubit and the field and inside the qubit system, yet with the rotating-wave approximation (RWA) [32–35]. Entanglement, as a fundamental quantum mechanical tool describing the nonlocal correlations between quantum objects, lies at the heart of quantum information sciences [36–38]. It is strongly expected that nontrivial population and entanglement dynamics will emerge in the ultrastrong-coupling regime where the RWA fails. For the Rabi model, a displaced Fock-state method [39] is developed to analytically predict the time evolution of the qubit's occupation probability in the case of strong coupling and large detuning. The key step is the adiabatic approximation, which nicely truncates the system Hamiltonian into a block diagonal form, and the resulting solutions are utilized to study the entanglement dynamics in a two-qubit system [25,40]. Specifically, a simple expression of the concurrence [41] for the two qubits is given analytically and entanglement sudden death appears even in the inhomogeneous coupling case. The circuit quantum electrodynamics (QED) architecture offers considerable potential for simulating such dynamics following an analog-digital approach [42].

This study was stimulated by the lack of an analytical analysis of bipartite entanglement in a multiqubit system in the ultrastrong-coupling regime. The typical model for this is the three-qubit Dicke model, characterized by a realistic realization of a Greenberger-Horne-Zeilinger (GHZ) state [43]. Recently, it has been shown that superconducting circuit technology allows the exploitation of dynamical Casimir effect physics as a useful resource for the generation of highly entangled states for multisuperconducting qubits [44]. It is thus desirable to demonstrate whether the sudden death of entanglement would survive the dissipative effects in the strong- and ultrastrong-coupling regimes [45]. Including the dissipation in the model is a hard computational task for numerical solution of the master equation since the mean photon number increases exponentially with time until it is balanced by the diminishing coupling strength to high-photon-number spaces. Here, we, on the other hand, show the robustness of the three-qubit GHZ and *W* states against the interaction and the energy exchange between the qubits and the field in the Dicke model, which could be of importance for future applications, e.g., in quantum cryptography [46,47], quantum computation [48], and quantum gates [49–51].

This paper is organized as follows. We solve the three-qubit Dicke model in a spin-3/2 subspace and derive the analytical eigensolutions by means of the adiabatic approximation in Sec. II. These results are applied to study of the population dynamics of three qubits coupled to, respectively, a Fock state and a coherent state of the oscillator in Sec. III. The spectrum of the multirevival signal is analyzed and compared to the numerical calculation without the adiabatic approximation. Then we explore the entanglement dynamics for three qubits starting from the GHZ or *W* state and the field in a coherent state and show the robustness of the GHZ state through the bipartite entanglement measure *I* tangle and the negativity in Sec. V. Finally, a brief summary is presented in Sec. VI.

II. EIGENSOLUTION OF THE THREE-QUBIT DICKE MODEL

We consider the three-qubit Dicke model described by the following Hamiltonian ($\hbar = 1$) [16,19,20]:

$$H = \omega_c a^\dagger a - \omega J_x + 2g(a^\dagger + a)J_z. \quad (1)$$

*ybzhang@sxu.edu.cn

Here $a^\dagger$ (a) is the creation (annihilation) operator of the single bosonic mode with frequency ω_c, ω denotes the qubit splitting, the constant g represents the coupling between the qubit and the field mode, and the total spin operator is the sum of the Pauli operators of the individual qubits, i.e., $J_i = \sum_{\alpha=1}^{3} \sigma_i^\alpha/2$ $(i = x,y,z)$. Note that J^2 commutes with the Hamiltonian, (1), i.e., $[J^2,H] = 0$, this provides a splitting of the eight-dimensional spin space into a quadruplet state space $j = 3/2$ and two doublet state spaces $j = 1/2$,

$$H = H^{3/2} \oplus H^{1/2} \oplus H^{1/2}, \tag{2}$$

which comes from three possible standard Young tableaux $\boxed{1}\boxed{2}\boxed{3}$, $\begin{array}{|c|c|}\hline 1&2\\\hline 3\\\cline{1-1}\end{array}$, and $\begin{array}{|c|c|}\hline 1&3\\\hline 2\\\cline{1-1}\end{array}$ in representation theory of permutation-group theory [52]. The three-qubit Dicke model thus decomposes into a system of one spin-3/2 and two spin-1/2 Rabi models [19]. While both models have been solved using the displaced Fock-space method [17,20,39] and Bargmann-space techniques [18,19], little attention has been paid to the analytical dynamics of the qubit occupation probability due to the cumbersome task of extracting the analytical solution in both formulations. Indeed the power series must be terminated in the transcendental function $G_\pm(x)$ [18] or the expansion of the wave function in terms of displaced Fock space should be truncated in a finite $N_{\rm tr}$ subspace [17,20].

Here, similar to the cases of the single-qubit [17,39] and two-qubit [25,40] Rabi models, we apply the adiabatic approximation to the numerical solutions when the frequencies of the qubits are much lower than the oscillator frequency $\omega \ll \omega_c$. In this displaced oscillator basis the Hamiltonian may be truncated to a block-diagonal form and the blocks solved individually. We confine ourselves in the following to a system with a four-dimensional spin subspace of $j = 3/2$, due to the fact that the Hamiltonian only couples states in this subspace, all interesting dynamics with the initial GHZ and W states in the three-qubit system prepared in the experiments is confined in this subspace, and best of all, this method is the most effective way to study analytically the dynamical properties of three qubits. The Hamiltonian $H^{3/2}$ reduces to a 4×4 block diagonal form, i.e., $H^{3/2} = \sum_{n=0}^{\infty} \oplus H_n$ with

$$H_n = \begin{pmatrix} \epsilon_{3/2}^n & \sqrt{3}\Omega_n & 0 & 0 \\ \sqrt{3}\Omega_n & \epsilon_{1/2}^n & 2\Omega_n & 0 \\ 0 & 2\Omega_n & \epsilon_{1/2}^n & \sqrt{3}\Omega_n \\ 0 & 0 & \sqrt{3}\Omega_n & \epsilon_{3/2}^n \end{pmatrix}, \tag{3}$$

where $\epsilon_m^n = \omega_c(n-\beta_m^2)$. The system is spanned by the the joint spin-field space $|3/2,m\rangle|n\rangle_{A_m}$, where $|j,m\rangle$ are eigenstates of J^2 and J_z with eigenvalues $j(j+1)$ and $m = -j,-j+1,\ldots,j$, respectively, and the displaced Fock states satisfy $A_m^\dagger A_m|n\rangle_{A_m} = n|n\rangle_{A_m}$, with $A_m = a+\beta_m$, $\beta_m = m\alpha$, and $\alpha = 2g/\omega_c$. The off-diagonal elements in the matrix are given by

$$\Omega_n = -\frac{\omega}{2} e^{-\frac{\alpha^2}{2}} \sum_{l=0}^{n} \frac{(-1)^{n-l} n!}{l![(n-l)!]^2} \alpha^{2(n-l)}. \tag{4}$$

It can be easily proved that the parity operator defined in the spin-3/2 subspace as $\Pi^{3/2} = \exp[i\pi(3/2 - J_x + a^\dagger a)]$, with eigenvalues $\kappa = \pm 1$, commutes with the Hamiltonian, i.e., $[H^{3/2},\Pi^{3/2}] = 0$. Accordingly, the Hilbert space splits into two mutually orthogonal subspaces with even and odd parities [19]. The four eigenstates of H_n are nondegenerate and can be classified uniquely by one quantum number. However, for numerical solutions beyond the adiabatic approximation, it is necessary to use the parity operator to classify the degeneracies that take place between levels of states with different parities. For consistency, we use parity invariance $[H_n,\Pi_n] = 0$, with Π_n an antidiagonal matrix $(-1)^n$adiag$[1,1,1,1]$, to further block diagonalize H_n as $H_n = \sum_{\kappa=\pm1} \oplus H_n^\kappa$, with

$$H_n^\kappa = \begin{pmatrix} \epsilon_{3/2}^n & \sqrt{3}\Omega_n \\ \sqrt{3}\Omega_n & \epsilon_{1/2}^n + 2\xi\Omega_n \end{pmatrix} \tag{5}$$

and $\xi = \kappa(-1)^n$. The energy levels are given by

$$E_n^{\kappa\pm} = n\omega_c + \xi\Omega_n - 5g^2/\omega_c \pm \theta_n^\kappa, \tag{6}$$

with $\theta_n^\kappa = \sqrt{(\xi\Omega_n + 4g^2/\omega_c)^2 + 3\Omega_n^2}$. The corresponding eigenstates in the spin-field space are

$$|\psi_n^{\kappa\pm}\rangle = d_n^{\kappa\pm}\left(c_n^{\kappa\pm},1,\xi,\xi c_n^{\kappa\pm}\right)^T, \tag{7}$$

with $c_n^{\kappa\pm} = \sqrt{3}\Omega_n/(\xi\Omega_n + 4g^2/\omega_c \pm \theta_n^\kappa)$ and $d_n^{\kappa\pm} = 1/\sqrt{2|c_n^{\kappa\pm}|^2+2}$. We restrict the analysis in the following to the case of $|\Omega_n| \gg 4g^2/\omega_c$ fulfilled by most experimental systems in the ultrastrong-coupling regime $g \leqslant 0.08\omega_c$, which enables us to achieve an analytical dynamics below. The eigenvalues are therefore simplified to

$$E_n^{\kappa\pm} = n\omega_c + (\xi \mp 2)\Omega_n, \tag{8}$$

and the corresponding eigenfunctions are

$$|\psi_n^{\kappa\pm}\rangle = \sqrt{\frac{2\mp\xi}{8}}\left(\frac{\sqrt{3}}{\xi\mp2},1,\xi,\frac{\xi\sqrt{3}}{\xi\mp2}\right)^T. \tag{9}$$

We observe that the parity κ and the photon number n in the displaced Fock state are independent of each other. This is due to the fact that in constructing the unitary transformation which brings the Hamiltonian into a block-diagonal form, (5), a phase difference $n\pi$ is introduced in the superposition of two displaced Fock states $|n\rangle_{A_m}$ in opposite directions so that the symmetric and antisymmetry superposition states of the corresponding bases have, respectively, even and odd parities. This situation resembles the parity of the ground state and the first excited state in the standard quantum tunneling model of a double-well potential.

III. POPULATION DYNAMICS

After a detailed discussion of the energy spectrum, we now turn to the study of the population dynamics of the qubits. In particular, we examine the dynamics with all three qubits being excited to the upper level $|eee\rangle$, while the initial state of the oscillator is prepared in the displaced Fock basis corresponding to it, i.e., $|\Psi(0)\rangle = |3/2,3/2\rangle|n\rangle_{A_{3/2}}$, which is expressed as the linear combination of the eigenvectors, (7):

$$|\Psi(0)\rangle = \sum_{\kappa,\tau} d_n^{\kappa\tau} c_n^{\kappa\tau} |\psi_n^{\kappa\tau}\rangle. \tag{10}$$

Then at a subsequent time t the probability of finding three qubits in the initial state $|3/2,3/2\rangle$ is easily obtained:

$$P_1(n,t) = |_{A_{3/2}}\langle n|\langle 3/2,3/2|\Psi(t)\rangle|^2. \tag{11}$$

Substituting the simplified eigensolutions, (8) and (9), into Eq. (11), we find that the probability is composed of three oscillating frequencies,

$$P_1(n,t) = \tfrac{1}{32}[10 + 15\cos(2\Omega_n t) + 6\cos(4\Omega_n t) + \cos(6\Omega_n t)], \tag{12}$$

while in the single- and two-qubit Rabi models we have, respectively, one and two frequencies dominating the evolution.

If, instead, initially the oscillator is displaced from a coherent state $|z\rangle$, i.e.,

$$|\Psi(0)\rangle = \sum_{n=0}^{+\infty} \frac{e^{-|z|^2/2} z^n}{\sqrt{n!}} |3/2,3/2\rangle |n\rangle_{A_{3/2}}, \tag{13}$$

which is the closest quantum state to a classical wave and more realistic for describing the oscillator, the probability of three qubits remaining in their initial state $|3/2,3/2\rangle$ is calculated by tracing over all Fock states as

$$P_1(z,t) = \langle 3/2,3/2|\mathrm{Tr}_F \rho(z,t)|3/2,3/2\rangle = \sum_{n=0}^{+\infty} p(n) P_1(n,t). \tag{14}$$

Here $\rho(z,t) = |\Psi(t)\rangle\langle\Psi(t)|$ is the density matrix of the system and the normalized Poisson distribution is defined as $p(n) = e^{-|z|^2}|z|^{2n}/n!$. Following the procedure established previously for the two-qubit model [40] by keeping only three terms, $l = n, n-1$, and $n-2$ in the summation of Ω_n and replacing the Poisson distribution with a Gaussian one for big enough $|z|$, we may reduce Eq. (14) into the analytical form

$$P_1(z,t) = \tfrac{1}{32}\mathrm{Re}[10 + 15S(t,\omega) + 6S(t,2\omega) + S(t,3\omega)], \tag{15}$$

with $S(t,\omega) = \sum_{k=0}^{+\infty} S_k(t,\omega)$. The collapse and revival of the probability $P_1(z,t)$, which are approximated with a fairly good accuracy by the sufficiently simple function $S_k(t,\omega)$, are obvious here, and the individual revival function

$$S_k(t,\omega) = h_k \exp(\Phi_{\mathrm{Re}} + i\Phi_{\mathrm{Im}}), \tag{16}$$

with height $h_k = (1+\pi^2k^2f^2)^{-1/4}$ and

$$\Phi_{\mathrm{Re}} = -\tfrac{1}{2}h_k^4(\mu-\mu_k)^2 f\alpha^2, \tag{17}$$

$$\Phi_{\mathrm{Im}} = \tfrac{1}{2}\tan^{-1}(\pi k f) + \mu(1-f) + 2\pi k|z|^2, \tag{18}$$

describes the evolution around the kth revival time $t_k^{\mathrm{rev}} = \mu_k/\omega$, where we have defined $f = |\alpha z|^2$, $\mu = \omega t e^{-\alpha^2/2}$, and $\mu_k = \pi k(f+2)/\alpha^2$. During each period $\Delta t = \pi(f+2)/\omega\alpha^2$, however, the signals in $S_k(t,2\omega)$ and $S_k(t,3\omega)$ revive twice and three times, respectively. We thus get three revival sequences in the evolution of the probability $P_1(z,t)$. The envelope and the fast oscillatory of the revival signal are determined by Φ_{Re} and Φ_{Im} respectively [40].

In Fig. 1, a comparison of the analytic formula derived for $P_1(z,t)$ and the numerical calculations is made in the parameter regime where the coupling strength is strong enough

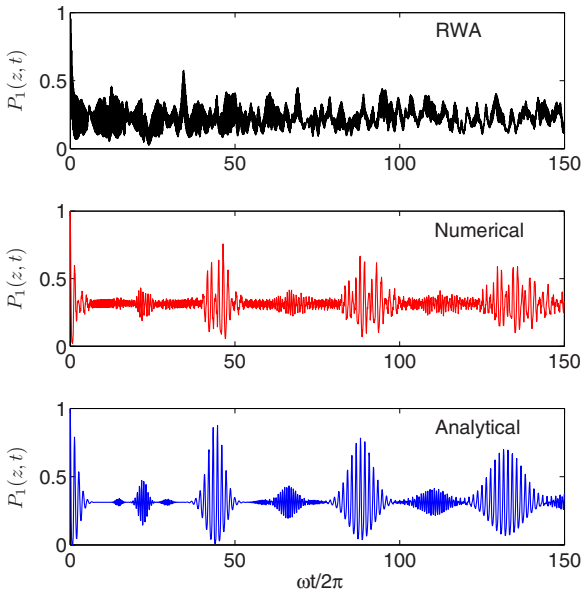

FIG. 1. Probability $P_1(z,t)$ of finding three qubits in the initial state $|3/2,3/2\rangle$ as a function of $\omega t/2\pi$ for $\omega = 0.15\omega_c$, $g = 0.08\omega_c$, and $z = 3$. Note that the breakup in the main revival peaks of the numerical evaluation, which comes from the ω-2ω-3ω beat note, is not included in the analytic calculation.

to invalidate the RWA. We see that with the time increasing the equilibrium value $10/32$, about which the revival signal oscillates, is smaller than $16/32$ in the single-qubit model and $12/32$ in the two-qubit model [40] due to the involvement of higher order harmonic signals in the probability. The width of the successive revival signals keeps increasing as $\delta\mu_k = \sqrt{1+\pi^2k^2f^2}/|z|\alpha^2$, which leads to the merging of the third harmonic signal into the first and second ones after several revival periods. The salient feature of the three-qubit model as demonstrated above is that the revival signals corresponding to the three oscillating terms $S(t,\omega)$, $S(t,2\omega)$, and $S(t,3\omega)$ produce a beat note of ω-2ω-3ω. The three revival sequences in the evolution of $P_1(z,t)$ are even clearer in the Fourier analysis $\bar{P}_1(z,\nu)$, defined as

$$\bar{P}_1(z,\nu) = \int_0^{+\infty} dt\, P(z,t) e^{-i2\pi\nu t}, \tag{19}$$

which is presented in Fig. 2. The spectral signals $\bar{P}_1(n,\nu)$ corresponding to the probability of the displaced Fock state are δ functions located at $2\Omega_n$, $4\Omega_n$, and $6\Omega_n$, respectively. The involvement of Fock states of many photons in the coherent state leads to a broad distribution of the spectral functions for $P_1(z,t)$ at a fundamental frequency $\omega^* = \omega e^{-\alpha^2/2}(1-|z|^2\alpha^2)$, which is 0.76ω for $g = 0.08\omega_c$ and $z = 3$, as well as at the second and third harmonics with decreasing magnitude. This contrasts the single and double revival sequences for the single- and two-qubit systems as a consequence of having only one and two Rabi frequencies, respectively, which have been shown in [40]. The analytical results reproduce the multiple revival sequences for the three-qubit model, except that breakups appear in the main and the second harmonic revival frequencies if no adiabatic approximation is made, which can be compared with the RWA case in [53]. We find that the RWA completely

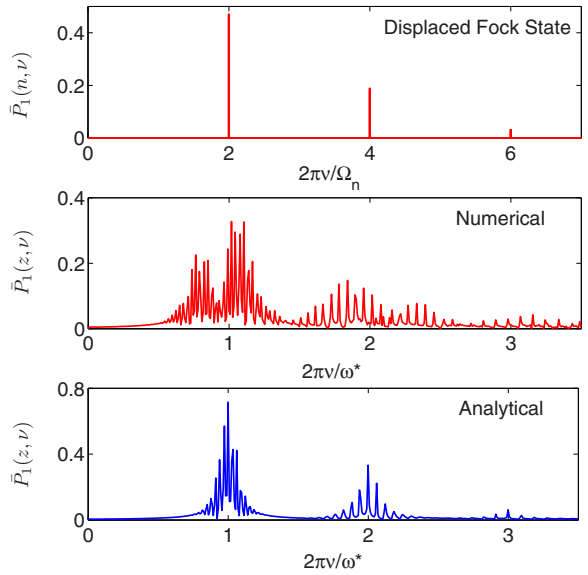

FIG. 2. Fourier analysis of the probability revival for the displaced Fock state (top) and displaced coherent state (middle and bottom panels for numerical and analytical calculations, respectively) of the oscillator with all three qubits being excited to the upper level. Three revival sequences in the dynamics produce a beat note of ω-2ω-3ω and the breakups in the fundamental and the second harmonic frequencies without the adiabatic approximation. The corresponding parameters are the same as in Fig. 1.

breaks down in the ultrastrong-coupling parameter regime considered here.

IV. ENTANGLEMENT BEHAVIORS

The entanglement properties of two identical qubits strongly coupled to a single-mode radiation field have recently been studied in [40] and [54], where the entanglement sudden death does appear in the numerical and analytic calculations. However, qualitative differences should arise in the case of the three-qubit system. It is widely accepted nowadays that entangled states of multiparticle systems are the most promising resource for quantum information processing [55–57]. Thus, it is highly desirable to explore the entanglement dynamics of the three-qubit Dicke model.

In this section we provide some easily computable formulas for the entanglement dynamics and compare the robustness of two typical three-qubit states. First, we consider that the field is initially in a coherent state $|z\rangle$ and the three qubits are initially in the form of a familiar GHZ state $\frac{1}{\sqrt{2}}(|eee\rangle + |ggg\rangle)$, i.e.,

$$|\Psi(0)\rangle = \frac{1}{\sqrt{2}}(|3/2,3/2\rangle + |3/2,-3/2\rangle)|z\rangle. \tag{20}$$

For small values of α, we may expand the state $|n\rangle$ in the displaced Fock space and the most important contribution in the summation over n comes from the terms with the same n, which is equivalent to taking $|n\rangle \approx |n\rangle_{A_m}$ [40]. This approximation gives the state at subsequent time t as

$$|\Psi(t)\rangle = \sum_{n,\kappa\tau} \sqrt{\frac{p(n)}{2}}(1+\xi) d_n^{\kappa\tau} c_n^{\kappa\tau} \left|\psi_n^{\kappa\tau}\right\rangle e^{-iE_n^{\kappa\tau}t}. \tag{21}$$

To examine the entanglement evolution of the system we calculate the reduced density matrix of the qubits by tracing over the quantum field

$$\rho_Q(t) = \sum_n \langle n|\Psi(t)\rangle\langle\Psi(t)|n\rangle, \tag{22}$$

which can be reduced to the matrix form

$$\rho_Q^G(t) = \frac{1}{4}\begin{pmatrix} 1 & 0 & \sqrt{3}S(t,2\omega) & 0 \\ 0 & 0 & 0 & 0 \\ \sqrt{3}S^*(t,2\omega) & 0 & 3 & 0 \\ 0 & 0 & 0 & 0 \end{pmatrix} \tag{23}$$

in the eigenbasis $|3/2,m\rangle_x$ of spin J_x. Note that only the term $S(t,2\omega)$ contributes to the reduced density matrix. This can be intuitively understood as a result of the classification of the energy spectrum by the parity operator Π: the initial state with the three qubits in the GHZ state has a definite parity depending on the photon number n. When we expand the initial state, (20), in the basis of eigenstates of $H^{3/2}$, the coefficients corresponding to the eigenstates with $\xi = -1$ are 0 in the adiabatic approximation. In Eq. (21) one must choose even $n = 2k$ for $\kappa = +$ or odd $n = 2k+1$ for $\kappa = -$. As a result, the time evolution of the reduced density matrix, (23), is uniquely characterized by the energy difference $|E_{2k}^{++} - E_{2k}^{+-}| = 4\Omega_n$ or $|E_{2k+1}^{-+} - E_{2k+1}^{--}| = 4\Omega_n$, leaving only one oscillation frequency determined by $S(t,2\omega)$.

The entanglement between the field and the qubits may be described by the I tangle

$$\tau_{FQ}(t) = 2\big(1 - \mathrm{tr}\big(\rho_Q^2\big)\big), \tag{24}$$

which is introduced in [58] and applicable to infinite-dimensional bipartite systems [34]. It runs from 0 for a product state to the maximum value $2(d-1)/d = 1.75$ with $d = \min(d_1,d_2)$ for a maximally entangled state, where d_1 and d_2 are, respectively, the dimensions of the three-qubit system and the photon field. The analytic expression for the reduced density matrix, (23), allows us to obtain the explicit formula

$$\tau_{FQ}^G(t) = \frac{3 - 3|S(t,2\omega)|^2}{4}. \tag{25}$$

In Figs. 3(a)–3(d), we plot the time evolution of the I tangle τ_{FQ}^G for various values of g. Should we adopt expression (7) for the eigenstates $|\psi_n^{\kappa\tau}\rangle$ and not take into account $|n\rangle \approx |n\rangle_{A_m}$, the adiabatic approximation produces an excellent agreement with the numerically exact solution in the ultrastrong-coupling regime as shown in Figs. 3(a)–3(d). The analytic result determined by formula (25) agrees well with the envelope of the numerically evaluated result but fails in describing the long-time behavior when the coupling strengths are sufficiently high, which is evident in Figs. 3(a)–3(d). The I tangle τ_{FQ}^G starts from 0 for the initial product state, (20), and undergoes periodic weakening and recovery, with the oscillation period getting smaller and smaller for increasing coupling strengths, which, however, could never reach the maximum entanglement value of the system. We see that the field-qubit entanglement exhibits collapse and revival and the analytic formula predicts correctly the main features of the individual entanglement revival signals.

The initially pure state of the qubits evolves into a mixed state described by the reduced density matrix ρ_Q^G in Eq. (23).

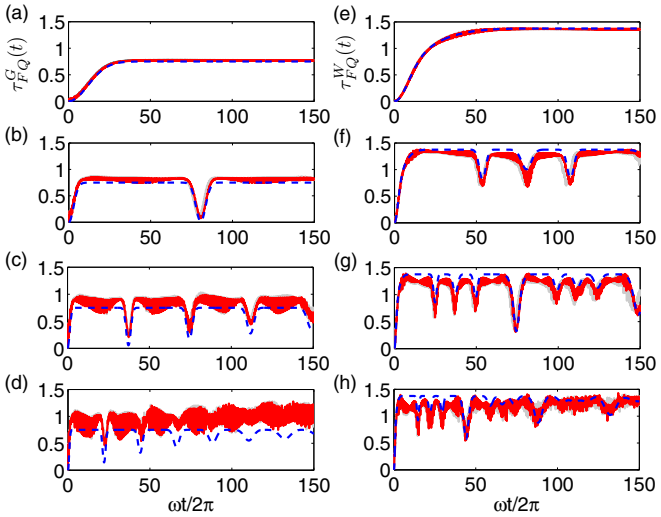

FIG. 3. Time evolution of the I tangle between the qubits and the light field with the initial GHZ (left) and W (right) states for $\omega = 0.15\omega_c$, $z = 3$, and different coupling strengths: (a,e) $g = 0.02\omega_c$, (b,f) $g = 0.04\omega_c$, (c,g) $g = 0.06\omega_c$ and (d,h) $g = 0.08\omega_c$, given by the numerical method (solid gray line), the adiabatic approximation (solid red line), and the analytical approach (dashed blue line).

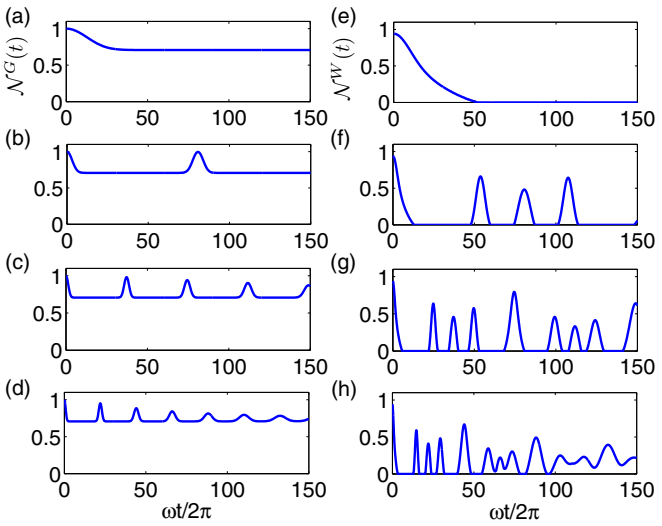

FIG. 4. Time evolution of the negativity inside the qubits with the initial GHZ (left) and W (right) states given by the analytical calculation. The corresponding parameters are the same as in Fig. 3.

We analytically study the entanglement between the qubits in the following. The measures of entanglement for mixed states depend on the pure-state decompositions; in this way the main difficulty is to find the minimization over all decompositions of the mixed state into pure states. However, our analytic method provides a particular case, where ρ^G_Q is a rank 2 mixed state of a qubit and a qudit in the basis of the three-qubit product states. Thus we may discuss the properties of the entanglement of a three-qubit system using the I tangle proposed by Osborne *et al.* [59]. As a good mixed-state entanglement measure for three qubits, the I tangle $\tau_{AB}(t)$ between one qubit (subsystem A) and the other two qubits (subsystem B) is given by the formula [59]

$$\tau_{AB}(t) = \mathrm{tr}(\rho_Q \tilde{\rho}_Q) + 2\lambda_{\min}\left[1 - \mathrm{tr}\left(\rho_Q^2\right)\right], \tag{26}$$

where the universal state inverter is defined as $\tilde{\rho}_Q = I_A \otimes I_B - \rho_A \otimes I_B - I \otimes \rho_B + \rho_Q$ with $\rho_A = \mathrm{tr}_B(\rho_Q)$ and $\rho_B = \mathrm{tr}_A(\rho_Q)$, and $\lambda_{\min}$ is the smallest eigenvalue of a real symmetric 3×3 matrix M as defined in [59] and [60]. A tedious yet straightforward calculation gives

$$M = \frac{1}{3(1+3|S(t,2\omega)|^2)} \times \begin{pmatrix} 2+2|S(t,2\omega)|^2 & 0 & \frac{4|S(t,2\omega)|}{\sqrt{3}} \\ 0 & \frac{-1-|S(t,2\omega)^2}{2} & 0 \\ \frac{4|S(t,2\omega)|}{\sqrt{3}} & 0 & \frac{-1+9|S(t,2\omega)|^2}{3} \end{pmatrix} \tag{27}$$

and $\lambda_{\min} = -(1+|S(t,2\omega)|^2)/(6+18|S(t,2\omega)|^2)$. Inserting this and the analytic expression (23) into Eq. (26) gives a very simple result for the bipartite entanglement

$$\tau^G_{AB}(t) = \frac{5+20|S(t,2\omega)|^2+7|S(t,2\omega)|^4}{8(1+3|S(t,2\omega)|^2)}. \tag{28}$$

An alternative way to quantify the entanglement of a bipartite system is the negativity, defined as [61]

$$\mathcal{N}(t) = 2\sum_i |\lambda_i|, \tag{29}$$

where λ_i are the negative eigenvalues of the partial transpose of ρ_Q with respect to system A or, equivalently, to system B. For ρ^G_Q, we find only one negative eigenvalue, which immediately gives

$$\mathcal{N}^G(t) = \sqrt{\frac{1+|S(t,2\omega)|^2)}{2}}. \tag{30}$$

The I tangle is then related to the negativity by

$$\tau^G_{AB}(t) = \frac{7[\mathcal{N}^G(t)]^4+3[\mathcal{N}^G(t)]^2-2}{4(3[\mathcal{N}^G(t)]^2-1)}. \tag{31}$$

The evolution of the negativity for three qubits is plotted in Figs. 4(a)–4(d). In contrast to the field-qubit entanglement $\tau^G_{FQ}(t)$, the negativity starts from the maximum value and then decreases to a finite steady value where entanglement sudden death is absent. When the field-qubit entanglement becomes rather weak this qubit-qubit entanglement increases rapidly to a large value, as can be seen in Figs. 3(a)–3(d) and Figs. 4(a)–4(d). From Eq. (31), the I tangle $\tau^G_{AB}(t)$ is found to be a monotonically increasing and decreasing function of the negativity $\mathcal{N}^G(t)$. It turns out that the decrease in $\tau^G_{FQ}(t)$ is directly related to the growth of $\tau^G_{AB}(t)$ in the form of Eq. (25) and Eq. (28), which predict correctly the time, height, and width of the individual entanglement oscillation. This indicates that the initial entanglement between the qubits withstands the

interaction and the energy exchange between the qubits and the field. In this way we provide for the first time an explicit analytical formula for the robustness of the GHZ state in the three-qubit Dicke model.

We now turn to entanglement dynamics of another three-qubit state, the W state $\frac{1}{\sqrt{3}}(|egg\rangle + |geg\rangle + |gge\rangle)$, which has also attracted considerable attention. We simply repeat the calculation in the preceding paragraphs with the GHZ state in the initial state $|\Psi(0)\rangle$ replaced by the W state. To monitor the time evolution of entanglement, we again need the explicit expression for the reduced density matrix of the qubits in the basis of spin J_x, given as

$$\rho_Q^W = \frac{1}{8}\begin{pmatrix} 3 & \sqrt{3}S(t,\omega) & -\sqrt{3}S(t,2\omega) & -3S(t,3\omega) \\ \sqrt{3}S^*(t,\omega) & 1 & -S(t,\omega) & -\sqrt{3}S(t,2\omega) \\ -\sqrt{3}S^*(t,2\omega) & -S^*(t,\omega) & 1 & \sqrt{3}S(t,\omega) \\ -3S^*(t,3\omega) & -\sqrt{3}S^*(t,2\omega) & \sqrt{3}S^*(t,\omega) & 3 \end{pmatrix}. \tag{32}$$

The reduced density matrix for the W state is obviously more complex than (23) for the GHZ state with the contributions from terms $S(t,\omega)$ and $S(t,3\omega)$. It nevertheless allows us to compute analytically the entanglement between the field and the qubits as

$$\tau_{FQ}^W(t) = \frac{22 - 7|S(t,\omega)|^2 - 6|S(t,2\omega)|^2 - 9|S(t,3\omega)|^2}{16}. \tag{33}$$

These three oscillating terms are clearly seen in the time evolution of the I tangle $\tau_{FQ}^W(t)$ for various g values as illustrated in Figs. 3(e)–3(h). Similarly to the GHZ state, it does not reach the maximum entanglement value but, on the whole, has a larger value than τ_{FQ}^G for the initial GHZ state.

Formula (26) for the I tangle is no longer applicable because the rank of the density matrix $\rho_Q^W(t)$ is larger than 2. We may, however, calculate the negativity for qubit-qubit entanglement in the W state using definition (29), and the result is shown in Figs. 4(e)–4(h). None of the eigenvalues of the partial transpose density matrix is negative in some periods of time, and sudden death of the qubit-qubit entanglement occurs in $\mathcal{N}^W(t)$ while the qubit-field entanglement $\tau_{FQ}^W(t)$ reaches its maximum. This phenomenon indicates that entanglement in the three-qubit GHZ state is surprisingly more robust than that in the W state against the interaction and the energy exchange between the qubits and the field, which is clearly depicted in Figs. 3 and 4. The findings here are in agreement with the robustness of multiparty entanglement under local decoherence modeled by partially depolarizing channels acting independently on each subsystem [62].

V. CONCLUSION

In conclusion, we have analyzed the population and entanglement dynamics of three qubits within the adiabatic approximation. It works very well in the ultrastrong-coupling regime under the assumption that the qubit frequencies are much lower than the field frequency. The remarkable feature of population dynamics in the three-qubit model is that the three revival sequences in the evolution of the probability produce a three-frequency beat note. Moreover, the analytic formulas of the I tangle for the pure state of a field-qubit system and the mixed state of a three-qubit system exhibit their excellence in entanglement characterization and distribution. This is the first study to present the robustness of the GHZ state in the form of the analytic expressions in the three-qubit Dicke model. The sudden death of entanglement is avoided in the three-qubit system with the initial GHZ state, which is qualitatively different from the two-qubit case studied in [25], [40], and [54]. The entanglement in the three-qubit GHZ state is shown to be more robust than that in the three-qubit W state. It is worth stressing that this method can be extended to the N-qubit Dicke model, but an increase in the detailed computational complexity should be noted. As a result, $N+1$ eigensolutions could be derived within the adiabatic approximation for the $N+1$–dimensional primitive block in the spin subspace of $j = N/2$, which results in as many as N oscillating frequencies for the W-like state in the dynamical evolution of the system. A practically relevant application of our result lies in the quantum information process with circuit QED, where three-qubit entangled states are involved.

ACKNOWLEDGMENTS

This work was supported by the NSF of China under Grants No. 11234008 and No. 11474189, the National Basic Research Program of China (973 Program) under Grant No. 2011CB921601, and the Program for Changjiang Scholars and Innovative Research Team in University (PCSIRT; No. IRT13076).

[1] J. Bourassa, J. M. Gambetta, A. A. Abdumalikov, Jr., O. Astafiev, Y. Nakamura, and A. Blais, Phys. Rev. A **80**, 032109 (2009).

[2] T. Niemczyk, F. Deppe, H. Huebl, E. P. Menzel, F. Hocke, M. J. Schwarz, J. J. Garcia-Ripoll, D. Zueco, T. Hümmer, E. Solano, A. Marx, and R. Gross, Nat. Phys. **6**, 772 (2010).

[3] A. Fedorov, A. K. Feofanov, P. Macha, P. Forn-Díaz, C. J. P. M. Harmans, and J. E. Mooij, Phys. Rev. Lett. **105**, 060503 (2010).

[4] P. Forn-Díaz, J. Lisenfeld, D. Marcos, J. J. Garc ía-Ripoll, E. Solano, C. J. P. M. Harmans, and J. E. Mooij, Phys. Rev. Lett. **105**, 237001 (2010).

[5] A. A. Anappara, S. De Liberato, A. Tredicucci, C. Ciuti, G. Biasiol, L. Sorba, and F. Beltram, Phys. Rev. B **79**, 201303(R) (2009).

[6] G. Günter, A. A. Anappara, J. Hees, A. Sell, G. Biasiol, L. Sorba, S. D. Liberato, C. Ciuti, A. Tredicucci, A. Leitenstorfer, and R. Huber, Nature **458**, 178 (2009).

[7] Y. Todorov, A. M. Andrews, R. Colombelli, S. De Liberato, C. Ciuti, P. Klang, G. Strasser, and C. Sirtori, Phys. Rev. Lett. **105**, 196402 (2010).

[8] M. V. Gustafsson, T. Aref, A. F. Kockum, M. K. Ekström, G. Johansson, and P. Delsing, Science **346**, 207 (2014).

[9] J. S. Pedernales, I. Lizuain, S. Felicetti, G. Romero, L. Lamata, and E. Solano, Sci. Rep. **5**, 15472 (2015).

[10] S. Felicetti, T. Douce, G. Romero, P. Milman, and E. Solano, Sci. Rep. **5**, 11818 (2015).

[11] S. De Liberato, Phys. Rev. Lett. **112**, 016401 (2014).

[12] S. Felicetti, G. Romero, D. Rossini, R. Fazio, and E. Solano, Phys. Rev. A **89**, 013853 (2014).

[13] P. Nataf and C. Ciuti, Phys. Rev. Lett. **107**, 190402 (2011).

[14] T. H. Kyaw, S. Felicetti, G. Romero, E. Solano, and L. C. Kwek, Sci. Rep. **5**, 8621 (2015).

[15] I. I. Rabi, Phys. Rev. **49**, 324 (1936); **51**, 652 (1936).

[16] R. H. Dicke, Phys. Rev. **93**, 99 (1954).

[17] T. Liu, K. L. Wang, and M. Feng, Europhys. Lett. **86**, 54003 (2009).

[18] D. Braak, Phys. Rev. Lett. **107**, 100401 (2011).

[19] D. Braak, J. Phys. B **46**, 224007 (2013).

[20] Q. H. Chen, Y. Y. Zhang, T. Liu, and K. L. Wang, Phys. Rev. A **78**, 051801 (2008).

[21] S. He, L. W. Duan, and Q. H. Chen, New J. Phys. **17**, 043033 (2015).

[22] J. Peng, Z. Ren, G. Guo, and G. Ju, J. Phys. A **45**, 365302 (2012).

[23] J. Peng, Z. Ren, D. Braak, G. Guo, G. Ju, X. Zhang, and X. Guo, J. Phys. A **47**, 265303 (2014).

[24] S. A. Chilingaryan and B. M. Rodríguez-Lara, J. Phys. A **46**, 335301 (2013).

[25] L. Mao, S. Huai, and Y. Zhang, J. Phys. A **48**, 345302 (2015).

[26] Q. H. Chen, L. W. Duan, and S. He, Ann. Phys. **355**, 121 (2015).

[27] Q.-T. Xie, S. Cui, J.-P. Cao, L. Amico, and H. Fan, Phys. Rev. X **4**, 021046 (2014).

[28] S. Cui, J. P. Cao, L. Amico, and H. Fan, arXiv:1504.04701.

[29] H. Zhong, Q. Xie, X. Guan, M. T. Batchelor, K. Gao, and C. Lee, J. Phys. A **47**, 045301 (2014).

[30] R. A. Robles Robles, S. A. Chilingaryan, B. M. Rodríguez-Lara, and R. K. Lee, Phys. Rev. A **91**, 033819 (2015).

[31] S. Felicetti, J. S. Pedernales, I. L. Egusquiza, G. Romero, L. Lamata, D. Braak, and E. Solano, Phys. Rev. A **92**, 033817 (2015).

[32] A. S. F. Obada, S. Abdel-Khalek, K. Berrada, and M. E. Shaheen, Physica A **392**, 6624 (2013).

[33] T. E. Tessier, I. H. Deutsch, A. Delgado, and I. Fuentes-Guridi, Phys. Rev. A **68**, 062316 (2003).

[34] M. Youssef, N. Metwally, and A. S. F. Obada, J. Phys. B **43**, 095501 (2010).

[35] C. E. López, G. Romero, F. Lastra, E. Solano, and J. C. Retamal, Phys. Rev. Lett. **101**, 080503 (2008).

[36] J. Preskill, J. Mod. Opt. **47**, 127 (2000).

[37] R. Islam, R. Ma, P. M. Preiss, M. E. Tai, A. Lukin, M. Rispoli, and M. Greiner, Nature **528**, 77 (2015).

[38] B. Hensen, H. Bernien, A. E. Dréau, A. Reiserer, N. Kalb, M. S. Blok, J. Ruitenberg, R. F. L. Vermeulen, R. N. Schouten, C. Abellán, W. Amaya, V. Pruneri, M. W. Mitchell, M. Markham, D. J. Twitchen, D. Elkouss, S. Wehner, T. H. Taminiau, and R. Hanson, Nature **526**, 682 (2015).

[39] E. K. Irish, J. Gea-Banacloche, I. Martin, and K. C. Schwab, Phys. Rev. B **72**, 195410 (2005).

[40] S. Agarwal, S. M. Hashemi Rafsanjani, and J. H. Eberly, Phys. Rev. A **85**, 043815 (2012).

[41] W. K. Wootters, Phys. Rev. Lett. **80**, 2245 (1998).

[42] A. Mezzacapo, U. Las Heras, J. S. Pedernales, L. DiCarlo, E. Solano, and L. Lamata, Sci. Rep. **4**, 7482 (2014).

[43] D. Greenberger, M. Horne, A. Shimony, and A. Zeilinger, Am. J. Phys. **58**, 1131 (1990).

[44] S. Felicetti, M. Sanz, L. Lamata, G. Romero, G. Johansson, P. Delsing, and E. Solano, Phys. Rev. Lett. **113**, 093602 (2014).

[45] D. Z. Rossatto, S. Felicetti, H. Eneriz, E. Rico, M. Sanz, and E. Solano, Phys. Rev. B **93**, 094514 (2016).

[46] J. Kempe, Phys. Rev. A **60**, 910 (1999).

[47] S. Y. Hao, Y. Xia, J. Song, and N. B. An, J. Opt. Soc. Am. B **30**, 468 (2013).

[48] L. Pedersen and C. Rangan, Quant. Info. Proc. **7**, 33 (2008).

[49] T. Monz, K. Kim, W. Hansel, M. Riebe, A. S. Villar, P. Schindler, M. Chwalla, M. Hennrich, and R. Blatt, Phys. Rev. Lett. **102**, 040501 (2009).

[50] A. Joshi and M. Xiao, Phys. Rev. A **74**, 052318 (2006).

[51] S. S. Ivanov, P. A. Ivanov, and N. V. Vitanov, Phys. Rev. A **91**, 032311 (2015).

[52] M. Dukalski and Y. M. Blanter, arXiv:1301.4857.

[53] Z. Deng, Opt. Commun. **54**, 222 (1985).

[54] Q. H. Chen, Y. Yang, T. Liu, and K. L. Wang, Phys. Rev. A **82**, 052306 (2010).

[55] C. H. Bennett, G. Brassard, C. Crepeau, R. Jozsa, A. Peres, and W. K. Wootters, Phys. Rev. Lett. **70**, 1895 (1993).

[56] M. A. Nielsen and I. L. Chuang, *Quantum Computation and Quantum Information* (Cambridge University Press, Cambridge, UK, 2000).

[57] R. Horodecki, P. Horodecki, M. Horodecki, and K. Horodecki, Rev. Mod. Phys. **81**, 865 (2009).

[58] P. Rungta, V. Bužek, C. M. Caves, M. Hillery, and G. J. Milburn, Phys. Rev. A **64**, 042315 (2001).

[59] T. J. Osborne, Phys. Rev. A **72**, 022309 (2005).

[60] G. Liberti, R. L. Zaffino, F. Piperno, and F. Plastina, Phys. Rev. A **76**, 042332 (2007).

[61] K. Zyczkowski, P. Horodecki, A. Sanpera, and M. Lewenstein, Phys. Rev. A **58**, 883 (1998).

[62] C. Simon and J. Kempe, Phys. Rev. A **65**, 052327 (2002).